




# Semantic Multiplexing

Mohammad Abdi , Francesca Meneghello , and Francesco Restuccia 

{abdi.mo,fr.meneghello,f.restuccia}@northeastern.edu  
Northeastern University, United States

## Abstract

Mobile devices increasingly require the parallel execution of several computing tasks offloaded at the wireless edge. Existing communication systems only support parallel transmissions at the bit level, which fundamentally limits the number of tasks that can be concurrently processed. To address this bottleneck, this paper introduces the new concept of *Semantic Multiplexing*. Our approach shifts stream multiplexing from *bits* to *tasks* by merging multiple task-related compressed representations into a single *semantic representation*. As such, Semantic Multiplexing can multiplex more tasks than the number of physical channels without adding antennas or widening bandwidth by *extending* the effective degrees of freedom at the *semantic* layer, without contradicting Shannon capacity rules. We have prototyped Semantic Multiplexing on an experimental testbed with Jetson Orin Nano and millimeter-wave software-defined radios and tested its performance on image classification and sentiment analysis while comparing to several existing baselines in semantic communications. Our experiments demonstrate that Semantic Multiplexing allows jointly processing multiple tasks at the semantic level while maintaining sufficient task accuracy. For example, image classification accuracy drops by less than 4% when increasing from 2 to 8 the number of tasks multiplexed over a 4×4 channel. Semantic Multiplexing reduces latency, energy consumption, and communication load respectively by up to 8×, 25× and 54× compared to the baselines while keeping comparable performance. We pledge to publicly share the complete software codebase and the collected datasets for reproducibility.

## 1 Introduction

Modern mobile devices need to continuously offload computing tasks (e.g., object detection, semantic segmentation) to edge servers to process high-data-rate multimedia inputs without prematurely exhausting their batteries. Such computing tasks need to be executed with ultra-low latency to avoid user discomfort [7]. While multiple-input multiple-output (MIMO) communication allows simultaneously transmitting (i.e., multiplex) multiple streams of bits in the same time/frequency resources, this does not suffice to provide adequate communication support for emerging applications (e.g., mobile virtual reality).

As detailed in Section 6, *existing task-driven compression and communication strategies can only process a single task at a time*. As such, they are fundamentally limited by the number of data streams currently supported by the wireless standards such as Wi-Fi and 5G. To make a real-world example, Apple’s virtual reality headsets are equipped with 12 cameras, among which 2 cameras are for high resolution video and generate 8K frames at 120 Hz each. This implies that 2 frames have to be compressed, transmitted and processed with an end-to-end delay of around 8 milliseconds without compromising the task accuracy [3]. Using H.265/HEVC compression and considering 8-bit color depth, each frame occupies 4 MB, corresponding to a data rate of 4 Gbps. State-of-the-art Wi-Fi 7 networks (802.11be) offer up to 2.875 Gbps per MIMO stream, meaning that at least two streams should be dedicated to each device, thus making the system not scalable [9].

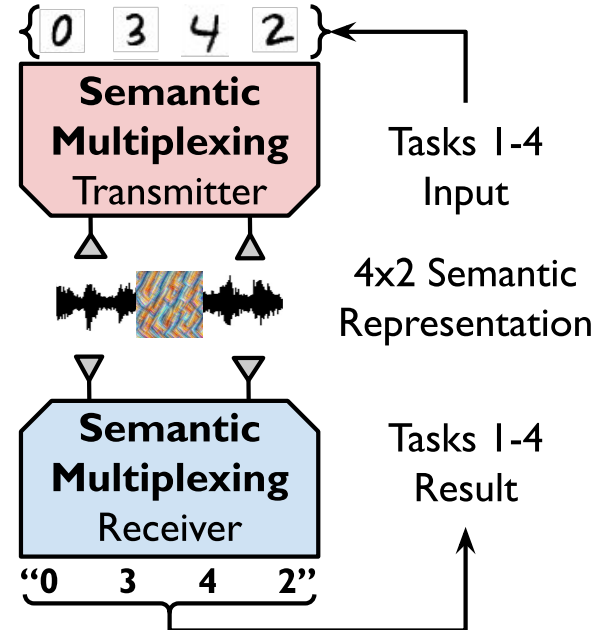


Figure 1: Example of semantic multiplexing four tasks into a single semantic representation spanning two physical streams. At the receiver, the representation is processed to execute the tasks in parallel.

To address this fundamental challenge, we introduce the new concept of *Semantic Multiplexing*, where we shift stream multiplexing from *bits* to *tasks*. By merging multiple task-related representations into a single *semantic representation* that is then multiplexed onto different physical data streams, Semantic Multiplexing *extends* the effective degrees of freedom at the *semantic* layer, without adding antennas or widening bandwidth while fully obeying Shannon capacity rules. Figure 1 shows an example where four digit recognition tasks (“0”, “3”, “4”, and “2”) are multiplexed and transmitted over two communication channels by semantically superimposing their representations into one physical signal. The latter is then semantically demultiplexed by the receiver to extract in parallel the output of the four tasks *at the same time*.

The fundamental technical advance behind Semantic Multiplexing is the integration of an additional semantic orthogonalization layer that can be on top of traditional systems such as MIMO. Critically, Semantic Multiplexing’s semantically-orthogonal streams can be *simultaneously processed and transmitted* while guaranteeing adequate final task performance for each multiplexed task. By creating *protected channels* for each task, Semantic Multiplexing enables both *computation and communication in superposition*, thus drastically reducing the overall task execution time.

**Technical Challenges.** The first key challenge is to devise a *task-agnostic* methodology to extract and map several latent representations into physical layer waveforms. For this reason, we propose a new information-theoretical framework where the joint design of communication and computation is enabled by the incorporation of the wireless channel model into the system as a non-learnable function (see Section 3.1). In stark opposition with prior work that optimizes communication and computing separately [5, 6], our design learns semantic coding in addition to the processing task end-to-end, thus effectively compensating for the distortion patterns caused by the channel while contributing to the processing for task execution.

The second challenge is to maintain orthogonality of the learned semantic representations with dynamic channels. As such, we introduce a new channel sounding methodology where pre-defined inputs are sent and processed as *semantic pilots* (see Section 3.3). As the task inference result for such pilots is known at the receiver, the Semantic Multiplexing transmitter and receiver are tuned considering the updated wireless channel and back-propagating the task loss through the corresponding computation channel. Prior work [1, 5, 6] only considers communication pilots, thus failing to properly adapt to changing wireless channel conditions as shown in Section 5.1. As Semantic Multiplexing is trained in an *end-to-end* manner, the over-the-air channel effects are leveraged

as part of the overall computation pipeline, contributing to the task execution.

### Summary of Novel Contributions

- We propose the first work that multiplexes several tasks on a single physical representation. Semantic Multiplexing orthogonalizes the task representations at the semantic level, thus enabling their joint processing and transmission to the receiver which demultiplexes the tasks and complete the processing to obtain the results. This way, Semantic Multiplexing drastically reduces the overall end-to-end latency due to task execution;
- We present a novel semantic channel sounding strategy for dynamically adapting the Semantic Multiplexing transmitter and receiver in the inference phase to preserve semantic orthogonality among computation and communication channels, accounting for the varying wireless environment;
- We extensively evaluate Semantic Multiplexing through real-world experiments. We prototyped Semantic Multiplexing using MIMO software-defined radios (SDRs) as the transmitter and receiver radio frontends and a Jetson Orin Nano board as the mobile device. We evaluated Semantic Multiplexing experimentally and compare it with state-of-the-art approaches in semantic communication (SemCom) on two tasks (image classification and sentiment analysis) to evaluate its efficacy on different input types (i.e., images vs text) and using different processing functions (Residual networks vs Transformers). Our experiments on system scalability show that Semantic Multiplexing allows multiplexing 8 tasks on 4 communication channels with a drop in accuracy of less than 2.5% with respect to multiplexing 4 tasks. Semantic Multiplexing decreases the end-to-end latency (communication plus computation) with respect to state-of-the-art semantic strategies by more than 7× on average and reduces energy consumption and communication load by more than 25× and 54× respectively.

### Summary of Impact

For the first time, this paper introduces and validates a new concept: *the number of tasks that can be semantically multiplexed in a communication system is greater the number of available physical streams*. As such, we believe this paper opens new and exciting research avenues at the intersection of machine learning and wireless networking.

## 2 Semantic Multiplexing

As depicted in Figure 1, Semantic Multiplexing semantically multiplexes multiple inputs for efficient transmission over wireless channels. Since the semantic transmission and reception pipelines are jointly optimized, Semantic Multiplexing is independent from the specific number of antennas at the transmitter and receiver. Specifically, the Semantic Multiplexing transmitter maps the task inputs into latent

representations to be directly transmitted through the available antennas, while the Semantic Multiplexing receiver processes the received signals to obtain the task outcomes.

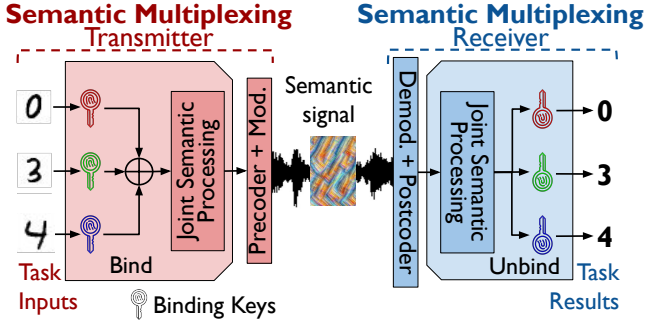


**Figure 2: Semantic Multiplexing transmitter and receiver. ‘Mod.’ and ‘Demod.’ stand for modulator and demodulator.**

The Semantic Multiplexing transmitter is summarized on the left side of Figure 2. The first operation consists of *binding* the task inputs using specific protected keys (see Section 2.1). This operation ensures that each input is processed in a separate protected subspace thus enabling semantic multiplexing [20, 22, 23]. Next, the bound key-value pairs are summed up element-wise to form a single compositional data structure that undergoes joint semantic processing (see Section 2.2). The output is then fed to learnable task-oriented precoding module, which allows Semantic Multiplexing to react quickly to sudden changes in the wireless channel. Based on channel state information (CSI), this module precodes the latent symbols by learning to optimize the end task performance (see Section 2.3). Finally, a non-trainable modulator generates the output waveform (see Section 2.4). At the Semantic Multiplexing receiver (see the right side of Figure 2), a non-trainable demodulator is combined with a data-driven task-oriented postcoding module and a joint semantic processing block to directly process the incoming waveforms to execute the task. The superposed task outputs are demultiplexed performing the unbinding operations using the corresponding keys.

As detailed in Section 3, the Semantic Multiplexing transmitter and receiver are jointly trained by adding a non-trainable stochastic model that represents the communication channel to link the transmitted and received latent representations. The rest of this section details the Semantic Multiplexing transmitter and receiver modules.

## 2.1 Binding/Unbinding

The binding mechanism used by Semantic Multiplexing is based on holographic reduced representations (HRR), which are implemented using circular convolutions [24]. More precisely, circular convolution is repeatedly applied between a

binding key and each input volume spanning across the feature maps. As a result, binding is translation-equivariant and maintains locality. The unbinding mechanism, on the other hand, is based on matrix binding of additive terms (MBAT) and is implemented through matrix multiplication [8]. The protection keys for binding and unbinding are initialized randomly and leaned during training to mitigate the interference between communication channels. For this, we leverage the fact that random tensors become quasi-orthogonal as their dimension increases. Therefore, we use unique high-dimensional keys to form quasi-orthogonal key-value pairs that can coexist and be processed concurrently. The binding keys are data-independent and are only linked to the specific multiplexed task input (i.e., computation channel). We refer interested readers to [16] for alternative binding mechanisms.

## 2.2 Joint Processing

After the binding operation, the task inputs undergo joint semantic processing to reduce latency and energy consumption. We model this operation as a differentiable function  $f_t(\omega_t)$  that processes the bound tasks toward the task execution. At the receiver, the joint processing, defined as a differentiable function  $f_r(\omega_r)$ , completes the task execution before the unbinding. Note that if the functions are not differentiable, they should be re-parametrized as differentiable functions, e.g., using [11, 13], to be included in the joint transmitter and receiver semantic optimization through loss backpropagation as detailed in Section 3.

Both learnable and heuristic functions can be used within Semantic Multiplexing depending on the task to be executed. If learnable, these modules help the precoding and postcoding in generating latent representations that are robust to the channel modifications and compensating for additional channel impairments at the receiver, as discussed in Section 2.3.

To help task execution, two additional disjoint processing steps can be integrated into the system. At the transmitter, before binding, the task inputs may be pre-processed to obtain higher-dimensional representations which further help isolate their processing once bound together. At the receiver, the unbound outputs may undergo another disjoint processing step to refine the task results. Whether to include these additional steps or not is a design choice and depends on the specific task to be executed and the computational power of the transmitter and receiver. As shown in Section 5.2, there is a tradeoff between the performance gain and the overall complexity of the system to account for in the system design.

**Example of Joint Processing Functions.** Our modeling applies to several tasks based on neural networks, including object detection with Residual networks [32] and text analysis with Transformer networks [18]. As shown in Figure 3,

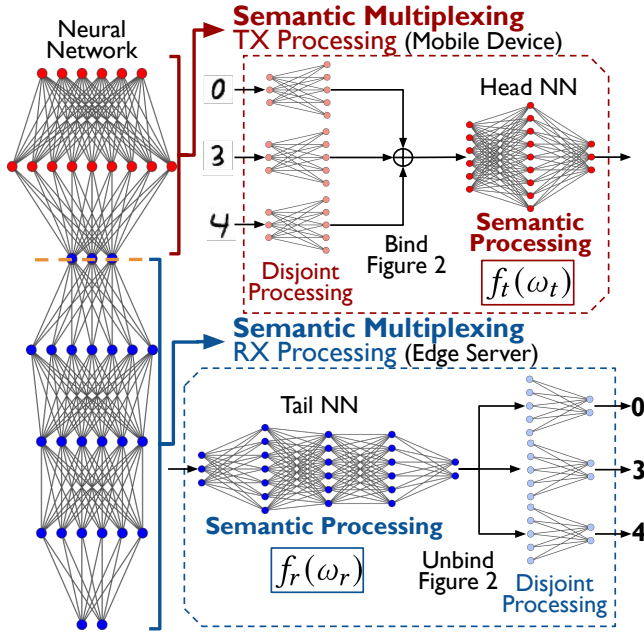


**Figure 3: Example of Semantic Multiplexing processing using a DNN for task execution.**

the deep neural network (DNN) responsible for task execution can be divided into two differentiable and learnable processing functions, which are then deployed at the Semantic Multiplexing transmitter ( $f_t(\omega_t)$ ) and receiver ( $f_r(\omega_r)$ ) [14, 17, 21]. At the transmitter, a portion of the head DNN, e.g., the first layer, can also be replicated for all inputs and used as the disjoint preprocessing function that helps the binding mechanism (see Figure 3, top). At the receiver, a similar strategy can be applied by isolating and replicating the last layer(s) for a final processing step on the unbound outputs to obtain the task results (see Figure 3, bottom). For example, in a classification task, the last linear (classifier) layer can be used.

### 2.3 Precoding/Postcoding

The precoding and postcoding allow quickly responding to channel variations maintaining sufficient task performance.

**Design Choices.** We design a learnable *stochastic precoder* since deterministic strategies result in a latent space where closer points do not necessarily associate with closer points in the task output space. As such, since deterministic models memorize an exact mapping between the latent and the output, a small perturbation of the latent – whether intentional (adversarial) or unintentional (channel distortions) – can change the task result drastically. Conversely, using a stochastic precoder with a customized loss function (see Section 3.2) allows imposing a prior distribution on the latent symbols, thus increasing the generalization ability. A

deterministic module is used for the learnable postcoder to simplify the formulation.

We examined three different approaches to design the precoder (the same applies “mirrored” to the postcoder). The most straightforward approach entails conditioning the entire transmitter processing function on the CSI, i.e., defining  $f_t(\omega_t|s)$  to process the bound task inputs. However, this increases the processing function complexity (e.g., the input layer size if a DNN is used as the processing function), incurring a high computation overhead on the transmitter, which is likely to be an energy-constrained mobile device as detailed in Section 1. Another option is to add another processing function (e.g., a separate neural network) to the transmitter to jointly process the output of the bound input processing (through function  $f_t(\omega_t)$ ) and the CSI. Although this option leaves the original transmitter function  $f_t(\omega_t)$  intact, it still leads to an increase in the transmitter computation load. Hence, we decided to use a dedicated precoding module to process the CSI separately, compute a task-oriented precoding tensor, and use it to transform the processed latent symbols to compensate for channel distortion. This option allows trading off representational power with reduced computation load.

**Design Details.** The precoder structure is depicted in the top side of Figure 4. As further detailed in Section 3, we assume that the conditional probability of latent symbols given the input has a complex Gaussian distribution, and the transmitter processing at the transmitter  $f_t(\omega_t)$  combined with the precoder extract the mean and covariance of this distribution. Let  $t$  be the bound and processed inputs obtained as output from  $f_t(\omega_t)$ . Since the Semantic Multiplexing precoder processes complex in-phase/quadrature (I/Q) symbols, tensor  $t$  is first converted to a complex tensor using the first part as the real and the second as the imaginary parts. The resulting tensor is split into multiple packets. The CSI, denoted by  $s$ , is fed to a linear layer with non-linear activation to compute the semantic precoding tensor for each packet. After applying the precoding (matrix multiplication) the packets are fed to other two linear heads with non-linear activations to extract the mean ( $\mu$ ) and the covariance ( $\Sigma$ ). The latent symbols generated by sampling a Gaussian distribution with these parameters and passed to the modulator described in Section 2.4 to generate the waveforms ready to be transmitted.

The postcoder (Figure 4, bottom) calculates the semantic postcoding tensor for each antenna similarly to the precoder obtaining the semantic postcoder tensor by processing the CSI  $s$  through a learnable linear transformation with a non-linear activation function. The corrupted latent symbols are postcoded using this tensor, processed through another



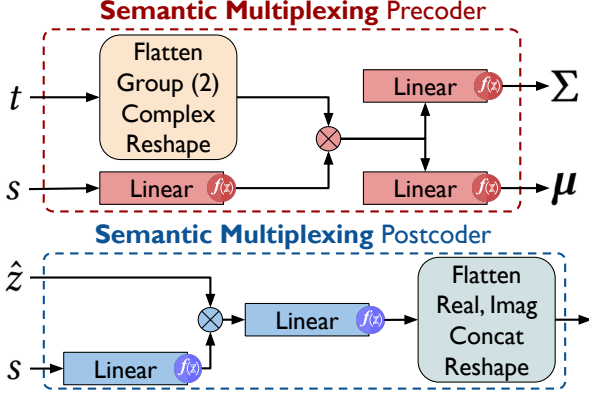


**Figure 4: Semantic precoding/postcoding in Semantic Multiplexing.**

linear layer with a non-linear activation, converted to real-valued feature maps and fed to the receiver processing block consisting of joint processing  $f_r(\omega_r)$ , unbinding and optional disjoint processing to obtain the tasks outcomes.

## 2.4 Modulation/Demodulation

At the transmitter, a modulator takes the latent symbols (from the precoder) in the frequency domain and transforms them to the time-domain baseband symbols, which can be up-converted to the carrier frequency and transmitted via a radio frontend. On the other hand, the received waveforms are down-converted to I/Q samples and further transformed to frequency-domain symbols by a demodulator. As such, the latent symbols transmission can be modeled as a matrix multiplication between the latent symbols at the modulator input (frequency domain) and the channel frequency response (CFR), followed by noise that provides the distorted latent symbols at the demodulator output. In this paper, in line with modern communication systems, we have realized the modulator/demodulator with direct and inverse fast Fourier transform (FFT) operations.

## 3 Mathematical Optimization

The Semantic Multiplexing system described in Section 2 is jointly trained to enable task-oriented precoding and postcoding that jointly optimize the communication and computation objectives. This is one of the key challenges in SemCom [5]. For this reason, previous work separately optimizes communication and computation thus obtaining a sub-optimal system without semantic multiplexing capabilities (e.g., see the MCR2/sm baseline [5, 6] in Section 5). In this section, we detail the new information-theoretical framework we developed to enable the combined training of all the learnable blocks in Semantic Multiplexing. One of the key innovation we introduce is the integration into the system of a channel model which describes how the signals

are modified during wireless propagation (see Section 3.1). Once derived the complete probabilistic model, we use the loss function formulated in Section 3.2 to jointly train the Semantic Multiplexing modules. In Section 3.3 we detail the strategies we designed and implemented to adapt dynamically the Semantic Multiplexing system to compensate for the changing wireless channel.

**Notation.** Random variables and their realizations are indicated by upper-case and lower-case letters, respectively.  $E\{X\}$  and  $H(X)$  denote the statistical expectation and entropy of variable  $X$ . The mutual information between  $X$  and  $Z$  is indicated by  $I(X; Z)$ , while  $H(Z|X)$  is the conditional entropy of  $Z$  given  $X$ . We use  $D_{KL}(p(x)||q(x))$  for the Kullback–Leibler (KL) divergence between  $p(x)$  and  $q(x)$  probability distributions. Finally,  $\mathcal{CN}(\mu, \Sigma)$  refers to the circularly-symmetric complex Gaussian distribution with mean  $\mu$  and covariance matrix  $\Sigma$ .

**Model Walkthrough.** The probabilistic model for Semantic Multiplexing is illustrated in Figure 5. We assume that the task input data  $x$  and their corresponding desired outputs  $y$  are generated by an information source having an underlying joint probability distribution  $p(x, y)$ . Let  $z$  be the latent symbols which are the frequency-domain input to the modulator. In the information-theoretic sense, we want these symbols to contain only the information needed to complete the task and obtain  $y$  at the receiver. The extraction of such symbols  $z$  from the inputs  $x$  and conditioned on the CSI ( $s$ ) for each packet  $p$  and subcarrier  $k$ , is modeled as sampling from the conditional probability  $p(z_{p,k}|x, s)$ . This probability is assumed to have a Gaussian distribution, which parameters are found combining the transmitter processing together with the stochastic precoder described in Section 2.3. To reduce the computational load, we adopt the mean-field assumption that the conditional probabilities for different packets and subcarriers in  $z$  are independent [4], i.e.,  $p(z|x, s) = \prod_{p=1}^P \prod_{k=1}^K p(z_{p,k}|x, s)$ . This is a common assumption in multi-carrier MIMO systems, where each packet and subcarrier is processed independently. Let  $f_{p,k}^{\mu}(x, s; \phi)$  and  $f_{p,k}^{\Sigma}(x, s; \phi)$  be the functions implemented by the combination of the transmitter processing ( $f_t(\omega_t)$ ) and the precoder for obtaining  $\mu$  and  $\Sigma$ , respectively, for packet  $p$  and subcarrier  $k$ , with  $\phi$  denoting the learnable parameters,  $p(z|x, s)$  writes as

$$p(z|x, s) = \prod_{p=1}^P \prod_{k=1}^K \mathcal{CN}(f_{p,k}^{\mu}(x, s; \phi), f_{p,k}^{\Sigma}(x, s; \phi)). \quad (1)$$

The conditional probability  $p(z_{p,k}|x, s)$  is approximated following two phases. At first, the transmitter precoding obtains  $p(t|x)$  conditioned on the inputs, where  $t$  is the processing output representation. Second, the stochastic precoder implements  $p(z_{p,k}|t, s)$  conditioned on  $t$  and the CSI,

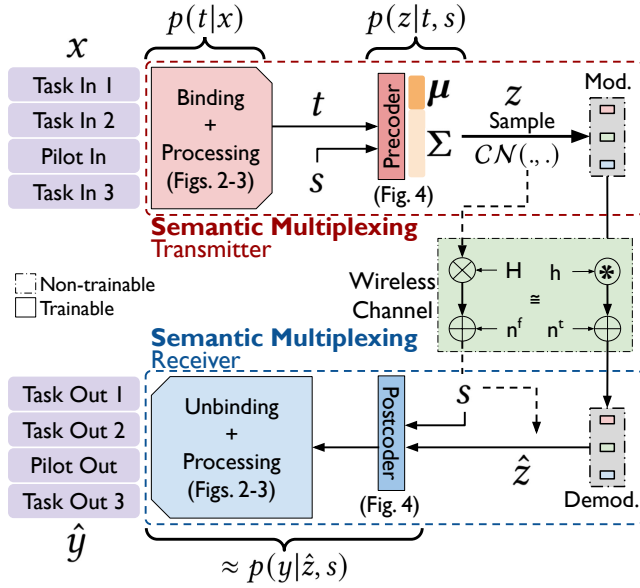


**Figure 5: Semantic Multiplexing probabilistic system model.**

obtaining  $p(z_{p,k}|x, s) = \int p(z_{p,k}|t, s)p(t|x)dt$ . After deployment, the transmitter modulates the symbols sampled from  $p(z|x, s)$  and transmits the waveforms over the channel.

The receiver collects the distorted signals and demodulates them into corrupted latent symbols  $\hat{z}$  which are then fed to the postcoder plus the receiver processing block ( $f_r(\omega_r)$ ) to finalize task inference and compute the results  $\hat{y}$ , using the function  $g(\hat{z}, s; \theta)$ , where  $\theta$  denotes the learnable parameters. The prediction of task outputs  $y$  from the corrupted latent symbols  $\hat{z}$  and conditioned on CSI  $s$  is modeled as sampling from a conditional probability  $p(y|\hat{z}, s)$ .

### 3.1 Modeling the Wireless Channel

During training, Semantic Multiplexing uses a stochastic model for signal propagation, representing the wireless channel between the transmitter and receiver in the frequency domain. The model accounts for the different number of antennas (one/multiple) at the transmitter and the receiver. We consider frequency-selective multi-path fading effects plus an additive complex white Gaussian noise. Both Rayleigh and Rician distributions are investigated for the fading. The CSI  $s$  modeling the channel includes both the CFR matrix  $H$  and the noise variance vector in the frequency domain denoted by  $\sigma^2$ . As shown in Figure 2, the latent symbols obtained at the transmitter are multiplied by the CFR  $H$ . Noise  $n^f \sim \mathcal{CN}(0, \sigma^2)$  is then added to obtain the corrupted latent symbols. Considering the constraints on the transmitter power, we normalize the peak power of the modulated signal to 1, resulting in an signal-to-noise ratio (SNR) of  $10 \log_{10} \frac{1}{\sigma^2}$ . The modulator, demodulator, and channel model

are non-trainable yet differentiable layers during the end-to-end training of Semantic Multiplexing, and are modeled by the equivalent conditional distribution  $p(\hat{z}|z, s)$ .

Accounting for the wireless transmission in Semantic Multiplexing is needed because the latent representations are transmitted as physical layer (PHY) waveforms. Hence, each latent collected at the receiver is a channel-distorted version of the transmitted representation. During the end-to-end training described in Section 3.2, Semantic Multiplexing identifies the distortion patterns caused by the channel and learns a custom channel coding strategy that robustifies the latent features against them. As such, Semantic Multiplexing performs channel coding on top of its processing task.

### 3.2 Formulation of Loss Function

As introduced before, from an information-theoretic viewpoint, our goal is to learn a latent  $Z$  that captures only the task-relevant information in  $X$  to predict  $Y$  at the receiver. Hence, we formulate the loss function used to train Semantic Multiplexing following the information bottleneck (IB) principle [27] as

$$\begin{aligned} \mathcal{L}_{IB} &= -I(\hat{Z}; Y|s) + \beta \cdot I(X; Z|s) \\ &= \mathbb{E}_{p(x, y)} \left\{ \mathbb{E}_{p(s)} \left\{ \mathbb{E}_{p(\hat{z}|x, s)} [-\log p(y|\hat{z}, s)] \right. \right. \\ &\quad \left. \left. + \beta \cdot D_{KL}(p(\hat{z}|x, s) || p(z)) \right\} \right\} - H(Y), \end{aligned} \quad (2)$$

where  $0 \leq \beta \leq 1$  is the weight controlling the efficiency-performance trade-off. By minimizing this loss function, we force  $Z$  to forget the unnecessary information in  $X$  by minimizing the mutual information  $I(X; Z|s)$ , and retain only the minimal sufficient statistics of  $X$  for expressing  $Y$  by maximizing the mutual information  $I(\hat{Z}; Y|s)$ . As a result, we can find the optimal  $Z$  which is maximally compressive about  $X$  while being maximally predictive about  $Y$ .

The conditional distribution  $p(\hat{z}|x, s)$  in Equation (2) is obtained as  $p(\hat{z}|x, s) = \int p(z|x, s)p(\hat{z}|z, s)dz$ , where  $p(z|x, s)$  is derived in Equation (1). However, computing the remaining distributions  $p(z)$  and  $p(y|\hat{z}, s)$  for high-dimensional data with arbitrary distributions is computationally prohibitive [1]. To overcome this issue, we leverage the variational information bottleneck (VIB) theory [2] to obtain a variational upper bound of the loss and the Monte Carlo sampling to derive an unbiased estimation of the expected values in the expression. Note that the precoder output is a distribution, and it should be sampled to obtain a realization. However, such sampling is not differentiable. Therefore, we use the reparameterization trick [15] to make Semantic Multiplexing trainable through loss backpropagation using a gradient descent algorithm. The details of this loss reformulation are included in Appendix A.

### 3.3 Dynamic Adaptation

After deployment and during testing, Semantic Multiplexing alternates between two operation modes to sound the wireless channel and adapt to changing conditions as summarized in Figure 6 and described next. While the first sounding is inherited from standard communication procedures, the second adaptation strategy is specifically designed for Semantic Multiplexing framework and has never been proposed before.

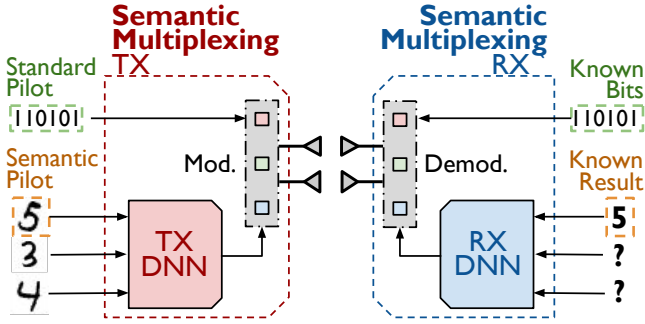


Figure 6: Standard and semantic channel sounding.

**Communication Pilots Transmission.** Each time before executing the inference, Semantic Multiplexing triggers the standard channel sounding procedure adopted for precoding in MIMO networks [10]. As such, the mobile device transmits a packet containing pilot symbols only. Using them, the edge server estimates the CSI  $s$  and feeds it back to the mobile device. The estimated CSI is used by the precoding and postcoding to make Semantic Multiplexing adapt to the varying wireless channel.

**Task-Oriented Pilots Processing.** During normal operation mode, Semantic Multiplexing randomly selects a computation channel to process task-oriented pilots. As the transmitter and receiver have to stay synchronized in selecting the index of such a computation channel, Semantic Multiplexing uses a hash function to obtain the index depending on the global time and a shared seed (established beforehand) without the need for explicit communication. The transmitter uses the selected channel to process an input with a known task output. For this, the transmitter device has to store a tiny subset of the training inputs as task-oriented pilots. Since the task result of the selected computation channel is known by the edge server, the corresponding loss can be calculated and backpropagated through that channel. Therefore, the Semantic Multiplexing transmitter and receiver DNNs are adapted in an end-to-end manner taking into account the updated MIMO channel model using the CSI estimated through communication pilots. This test-time adaptation procedure maintains isolation between different computation and communication channels.

## 4 Experimental Prototype

We developed an end-to-end prototype illustrated in the upper part of Figure 7, where we use a Jetson Orin Nano board powered by a 32-tensor-core NVIDIA Ampere GPU and a 6-core ARM Cortex-A78AE CPU as the (energy-constrained) transmitter. A workstation equipped with a 432-tensor-core NVIDIA A100 GPU and a 12-core Intel Xeon Silver 4410Y CPU is considered as the receiver. Millimeter-wave (mmWave) SDRs are used as the transmitter and receiver. The SDRs operate at 60 GHz with a bandwidth of 1 GHz and are equipped with 8 digitally-controlled RF chains each, thus supporting fully digital  $8 \times 8$  mmWave communications. The Jetson Orin Nano board is connected to the transmitter radio while the other SDR is connected to the receiver. The prototype has been deployed in a conference room, as shown at the bottom of Figure 7. We conducted the experiments both with and without the absorber foams placed at 1.5 m distance from the radios, corresponding to non-line-of-sight (NLoS) and line-of-sight (LoS) scenarios (Rayleigh and Rician fading).

During training, we consider 20 dB SNR to determine the additive noise variance in the probabilistic model while the CFR is collected from the experimental setup and changed at every epoch. We incorporated an orthogonal frequency division multiplexing (OFDM) modulation scheme with an FFT size of 1024, where 800 subcarriers are used out of 1024, while the rest are left unused as guard bands. ReLU is used as the non-linear activation function in the precoder and post-coder. The trade-off parameter in Equation 4 is set to  $\beta = 10^{-4}$ . In the testing phase and during adaptation, all the parameters are frozen, except for the precoding and postcoding parameters plus the binding and unbinding keys.

### 4.1 Processing Tasks

We tested Semantic Multiplexing with image classification and sentiment analysis tasks to evaluate the efficacy of Semantic Multiplexing on different input types (i.e., images vs text) and using different processing functions (Residual networks vs Transformers).

**Image classification.** Consistent with existing work, we considered CIFAR-10, CIFAR-100, and SVHN. CIFAR-10 and CIFAR-100 contain 50,000 training images and 10,000 testing images each, distributed evenly among 10 and 100 classes, respectively. SVHN comprises 73,257 training images and 26,032 testing images across 10 classes. All datasets have RGB input channels. Data augmentation was consistently applied to the training set through random horizontal flips, random cropping, and normalization. WideResNet DNNs were selected for image classification. Specifically, we selected the learning models WRN-28-10, WRN-16-8, and WRN-10-4 [32], where the first and second numbers in the name indicate the depth (number of layers) and width (number of kernels)



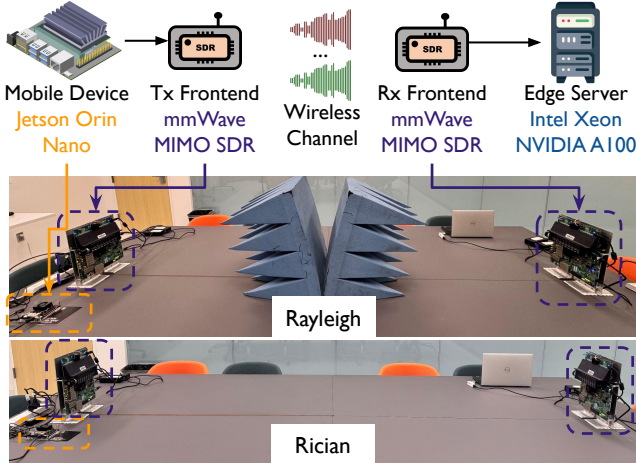


**Figure 7: Experimental setup for real-world evaluation of Semantic Multiplexing in a conference room in NLoS (Rayleigh fading, with the absorbers) and LoS (Rician fading).**

of each model. The larger architectures provide improved performance at the cost of increasing computational and memory load. We divide each backbone after the first ResNet block and deployed the one-block head DNN on the mobile device (joint processing function  $f_i(\omega_i)$  in Section 2.2) and the remaining tail DNN at the edge server ( $f_r(\omega_r)$ ), as depicted in Figure 3.

**Sentiment analysis.** We considered the second task in the long range arena (LRA) Transformers benchmark on text analysis [26]. We used the IMDb reviews dataset, which contains 50,000 movie reviews for binary sentiment classification [18]. The authors of the dataset defined a set of 25,000 highly polar movie reviews for training and 25,000 for testing. We used the Transformer architecture in [20] as the signal processing function for sentiment classification. Specifically, the selected architecture consists of 6 attention blocks with 8 heads each. This architecture presents an additional challenge with respect to the WideRedNet as the binding and unbinding processes should be sequentially performed for each of the of the attention blocks to enable task multiplexing. We deployed the first attention layer until the multi-layer perceptron before the unbinding at the transmitter, while the unbinding for the first block and the remaining attention blocks have been deployed at the receiver.

For both tasks, at the transmitter, the first convolutional layer is cloned for each of the task inputs as a preliminary disjoint processing to improve the separation in the semantic space enforced by the binding mechanism. At the receiver, the last linear (classifier) layer is duplicated for all the outputs. Each classifier is fed with one of the unbound values and returns the associated task result.

## 4.2 Baseline Approaches

We consider four baselines. For baseline naming we use the convention ‘MethodName/xy’, where ‘x’ and ‘y’ identify the computation and communication strategy, respectively, adopted by the method, which can be multiplexed (letter m) or not (letter s). Notably, Semantic Multiplexing is the first approach in the literature proposing to multiplex both computation and communication. In the following, we describe the baselines by grouping them into two categories. The first includes approaches that use semantic at the application layer and transmit data using full protocol stack, while the approaches in the second directly obtain PHYrepresentations.

**Full-Stack SemCom:** These approaches use IEEE 802.11 (Wi-Fi) to transfer latent representations. Specifically, the latent floating-point features for each batch of images are converted into their bit representations and divided into application layer protocol data units (PDUs) based on a suitable maximum transmission unit (MTU) size. The PDUs are encapsulated using transmission control protocol (TCP) and the Wi-Fi data link layer to form physical-layer bits. The I/Q symbols are obtained using a quadratic phase-shift keying (QPSK) modulation scheme and fed to an OFDM block to be further transmitted using the radio. The retransmission mechanisms employed at different layers of the protocol stack allow these methods to maintain performance with different communication channel conditions, at the cost of increasing end-to-end latency and mobile energy consumption. We consider the following baselines:

- **MNet/ms:** We used the method proposed in [20] to build MIMO-DNNs based on WideResNets. Then, we applied the algorithm in [14] to divide the DNNs between the transmitter and the receiver. The first layer of the DNN is deployed on the transmitter, while the rest is executed on the receiver.

- **BF/ss:** The authors in [19] reduced the amount of transferred data learning a compressed latent representation in single-input DNNs by reducing the width of the last convolutional layer in the first WideResNet block and other affected layers. A two-stage training utilizing knowledge distillation (KD) is used to compensate for accuracy drop. We followed the same approach and used 9 and 3 kernels as the reduced width, indicated as BF-9/ss and BF-3/ss, respectively.

**Physical Layer SemCom:** In these approaches, the latent symbols are already channel-encoded. We implemented the packet detection and synchronization similarly to Wi-Fi. These methods implicitly compensate for channel impairments regardless of the wireless condition and without relying on retransmissions. We consider two baseline methods:



- **MCR2/sm**: In [5, 6], a MIMO SemCom system uses linear precoding and postcoding blocks similar to those in traditional communication systems, which are updated through an iterative algorithm. Class-wise separability is adopted as a surrogate measure for classification accuracy. The entire DNN up to the penultimate layer is executed at the transmitter which sends only the class probabilities to the receiver. While in the provided implementation a fixed CSI is used, we made it adaptive to have a fair comparison with Semantic Multiplexing.

- **PhyDNN/ss**: Abdi et al. [1] proposed modifying and fine-tuning an already-trained DNN to deploy it directly in the PHY layer producing single-stream transmissions. Their key modification involves introducing a codebook into the DNN to produce discrete latent symbols compatible with a given digital modulation scheme. To utilize this approach as a baseline, we applied it to WideResNet models, generating OFDM symbols at the output of the first layer.

## 5 Experimental Results

In Section 5.1, we study the performance of Semantic Multiplexing in terms of task accuracy. We show that the joint design of computation and computation does not lead to consistent performance degradation with respect to full-stack approaches and allow increasing accuracy for PHY strategies. In Section 5.2, we study the scalability of Semantic Multiplexing when multiplexing an increasing number of task inputs (i.e., computation channels). The results show that Semantic Multiplexing allows multiplexing more tasks than communication spatial streams. Finally, in Section 5.3 we comprehensively evaluate Semantic Multiplexing against baselines based on latency, energy consumption, communication and computation efficiency. The adaptation capability of Semantic Multiplexing under variations in the communication environment is also evaluated and compared with MCR2/sm to demonstrate the effectiveness of the proposed techniques—namely, precoder/postcoder response and task-oriented pilot transmission—in addressing short-term and long-term changes, respectively. All results correspond to processing a full 64-element batch. In experiments involving MIMO computation-enabled methods, the metrics are normalized by the number of multiplexed tasks, providing average values per input. In the following, will use **SM** in tables and figures to indicate our Semantic Multiplexing approach.

### 5.1 Task Accuracy

We multiplexed 4 tasks on 8 communication channels for image classification while 2 tasks were multiplexed on 8 communication channels for sentiment analysis. This setting allows a fair comparison of Semantic Multiplexing with the baselines which do not provide multiplexing support for

more tasks than physical streams. Note that full-stack baselines achieve identical accuracy in both LoS and NLoS, as the use of a communication standard guarantees the exact representation transmitted from the mobile device is received at the edge server. Thus, their results are channel-independent and reported only once. In contrast, latent representations in methods MCR2/sm, PhyDNN/ss, and Semantic Multiplexing are directly influenced by the wireless environment.

**Image classification.** Table 1 presents the classification accuracy considering the different versions of the WideResNet and using CIFAR-10. The evaluation on CIFAR-100 and SVHN is reported in Appendix B. The results show that Semantic Multiplexing delivers consistently high performance across all architectures and conditions. Specifically, it outperforms other approaches under both LoS and NLoS conditions. The advantage over MCR2/sm stems from the joint optimization of communication and computation while MCR2/sm’s linear precoder and postcoder are separately designed and thus sub-optimal. Likewise, the performance gain over PhyDNN/ss is because the latter relies on a fixed codebook, which cannot adapt to varying channel conditions. Semantic Multiplexing exhibits remarkable robustness, with the average performance drop of less than 4% when transitioning from LoS to NLoS, e.g., from 94.48% to 90.92% using WRN-28-10. This represents an improvement of 4.61% and 4.16% over MCR2/sm in the same conditions. Semantic Multiplexing robustness is further evident in challenging scenarios – even with the smallest architecture (WRN-10-4), Semantic Multiplexing achieves 85.76% accuracy in NLoS, surpassing the performance of MCR2/sm (85.36%) and PhyDNN/ss (85.25%) under favorable LoS conditions by 0.40% and 0.51%, respectively. While full-stack methods achieve highest accuracy, it comes at the cost of increased latency as detailed in Section 5.3. In contrast, Semantic Multiplexing attains comparable performance (93.69% with WRN-16-8) with substantially lower latency.

**Table 1: Image classification. Experimental evaluation of Semantic Multiplexing and baselines for different DNNs on CIFAR-10.**

WRN-28-10	MNet	BF-9	BF-3	MCR2	PhyDNN	SM
LoS	94.74 %	96.88 %	96.42 %	89.87 %	92.50 %	94.48 %
NLoS				86.76 %	88.23 %	90.92 %
WRN-16-8	MNet	BF-9	BF-3	MCR2	PhyDNN	SM
LoS	93.86 %	95.96 %	95.44 %	89.17 %	91.85 %	93.69 %
NLoS				84.97 %	87.05 %	89.46 %
WRN-10-4	MNet	BF-9	BF-3	MCR2	PhyDNN	SM
LoS	87.71 %	91.38 %	90.13 %	85.36 %	85.25 %	87.29 %
NLoS				83.40 %	83.34 %	85.76 %

**Sentiment analysis.** Table 2 shows the results of the accuracy in the binary classification of sentiments using the

Transformer architecture for text processing. The results follow the same trend discussed for image classification: Semantic Multiplexing is the most effective approach among the PHY SemCom strategies and achieve accuracy values comparable to the ones of full protocol stack baselines.

**Table 2: Sentiment analysis. Experimental evaluation of Semantic Multiplexing and the baselines for the Transformer on LRA.**

Transformer	MNet	BF-9	BF-3	MCR2	PhyDNN	SM
LoS	64.39 %	66.06 %	65.81 %	60.93 %	61.04 %	64.02 %
NLoS	64.39 %	66.06 %	65.81 %	59.44 %	59.52 %	62.83 %

## 5.2 Semantic Scalability

We evaluate the scalability of Semantic Multiplexing in terms of how the task accuracy varies based on the number of multiplexed tasks.

Figure 8 reports an extensive scalability evaluation performed using the image classification task and testing the performance of the different DNNs on the three considered datasets. In general, the results demonstrate that Semantic Multiplexing can multiplex more tasks than the number of physical streams supported by a given transceiver hardware, without noticeable degradation in individual task performance. More in detail, by comparing the results in the first three subplots – obtained considering 4 communication streams and multiplexing 2, 4, 6 and 8 tasks at a time – we notice that the performance drop is linked with the difficulty of the task (e.g., CIFAR-10 vs CIFAR-100) and the complexity of the DNN used for processing (e.g., WRN-28-10 vs WRN-10-4). For example, Figure 8a shows that WRN-28-10 allows multiplexing 8 tasks guaranteeing a task accuracy of 93.09% which is only 4% less than the one achievable multiplexing 2 tasks (97.01%), while reducing latency by 4× thanks to semantic multiplexing (8 streams are simultaneously processes instead of only 2). The same trend is visible in Figures 8b-c, with accuracy decrease rates that are dataset- and DNN-specific. For example, for the more complex CIFAR-100 dataset (Figure 8b), accuracy drops by about 10% when multiplexing 8 streams (71.19%) instead of 2 (81.29%) and its values are consistently smaller than the one achievable with the simpler 10-class datasets.

Finally, in Figure 9, we analyze Semantic Multiplexing scalability on the sentiment analysis task which uses Transformers. The evaluation have been performed considering 2 communication channels. The results are promising also in this case, with less than 10% accuracy drop when increasing the number of multiplexed tasks from 2 to 8.

**Disjoint Preprocessing.** In Table 3, we investigate the impact of the disjoint processing – applied at the transmitter to the task inputs before binding (see Section 2.2, Figure 3)

– on the Semantic Multiplexing scalability. Specifically, we compared the performance of Semantic Multiplexing on image classification with CIFAR-10 when doubling the number of kernels in the convolutional layer used for the disjoint processing. The results are obtained using 4 communication channels while multiplexing 6 and 8 tasks and show that increasing the number of kernels ameliorates performance, especially when increasing the number of tasks to be multiplexed. This confirms that applying a preprocessing step before the binding helps enforcing orthogonality among the computation channels and can be optimized based on the specific task and hardware constraints.

**Table 3: Image classification. Semantic Multiplexing accuracy for different DNNs on CIFAR10 changing the number of kernels in the disjoint processing for 6 and 8 multiplexed tasks.**

WRN-28-10		
	1× Kernels	2× Kernels
Tasks = 6	94.32 %	96.21 %
Tasks = 8	93.09 %	95.82 %
WRN-16-8		
	1× Kernels	2× Kernels
Tasks = 6	92.85 %	93.93 %
Tasks = 8	90.74 %	91.82 %
WRN-10-4		
	1× Kernels	2× Kernels
Tasks = 6	84.57 %	88.48 %
Tasks = 8	79.25 %	80.52 %

## 5.3 Resource Efficiency

We evaluated Semantic Multiplexing against the other baselines on the CIFAR-10 dataset for the computational analysis. We considered 8 communication channels and multiplexed 4 task inputs for this evaluation. We obtain the following figures of merit to evaluate the complexity (i) end-to-end execution time; (ii) energy consumption at the mobile device; (iii) total number of transmitted symbols from the mobile device to the edge server (communication efficiency); (iv) total number of DNN parameters and operations performed by the mobile device (computation efficiency). For latency and energy measurements, evaluations were performed over 100 full executions (epochs) of the test set. To obtain reliable estimates of energy consumption, instantaneous power readings were sampled more than 1,000 times during data acquisition and averaged.

**End-to-End Latency.** The end-to-end latency accounts for (i) computation time on the mobile device (head DNN); (ii) communication latency of sending latent representations; (iii) inference time on the edge server (tail DNN). Figure 10a, 10b, and 10c report the breakdown of latency results for WRN-28-10, WRN-16-8, and WRN-10-4 architectures, respectively, under LoS and NLoS scenarios. For methods employing superposition and precoding at the mobile device, and

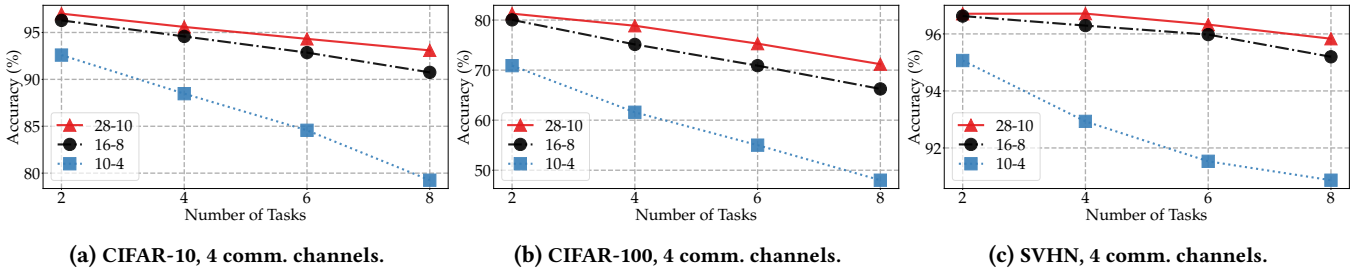


**Figure 8: Image classification. Scalability evaluation with 2 and 4 communication channels and varying the number of multiplexed task inputs. ‘WRN-’ is omitted in the legend for the different DNNs for clarity.**

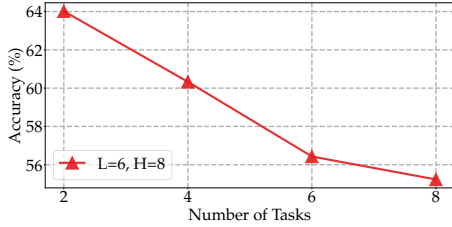


**Figure 9: Sentiment analysis. Scalability evaluation with 2 communication channels and varying the number of multiplexed task inputs.**

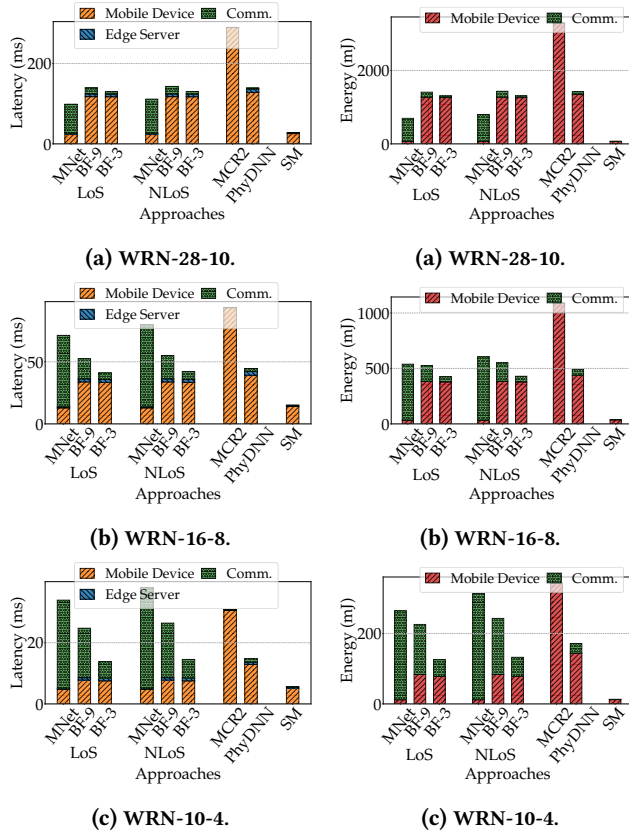


**Figure 10: Breakdown of end-to-end latency.**

**Figure 11: Mobile device energy consumption.**

postcoding and decomposition at the edge server, the latency overhead of these modules is included in the reported inference times. Across all settings, Semantic Multiplexing consistently shows lower latency compared to all baselines, including both full protocol stack and PHY approaches.

Communication latency is the primary bottleneck for full protocol stack approaches especially in NLoS scenarios, where frequent retransmissions further increase delay. By transmitting task-relevant features directly at the PHY, Semantic Multiplexing avoids such an overhead. For instance, MNet/ms incurs up to 930× higher communication latency than Semantic Multiplexing in NLoS. Although PhyDNN/ss also operates at the PHY and maintains consistent latency across channel conditions, its single-stream transmission limits efficiency. By leveraging semantic multiplexing, we achieve a 32× reduction in average latency with respect to PhyDNN/ss, since it can transmit semantic features in parallel across multiple streams.

Beyond communication efficiency, Semantic Multiplexing also achieves a notable reduction in computation latency compared to PHY baselines. Unlike MCR2/sm and PhyDNN/ss, Semantic Multiplexing supports multi-task semantic processing, lowering computation latency by up to 11.3× and 5.0×, respectively.

Overall, averaged across all backbones and channel conditions, Semantic Multiplexing reduces the total latency by 4.46× over MNet/ms, 4.55× over BF-9/ss, 3.82× over BF-3/ss, 8.53× over MCR2/sm, and 4.09× over PhyDNN/ss.

**Energy Consumption.** We evaluate the energy consumption, including (i) energy consumption during transmitter-side DNN execution; (ii) energy consumed to communicate the latent. As illustrated in Figure 11a, 11b, and 11c, the overall energy footprint varies significantly with the DNN size and the communication environment. Full-stack baselines incur high communication energy, especially in NLoS, while MCR2/sm shows high computation energy due to its heavy processing on the mobile device.

In contrast, Semantic Multiplexing maintains a consistently low energy profile across all architectures. It achieves up to 187.51× lower communication energy than full-stack

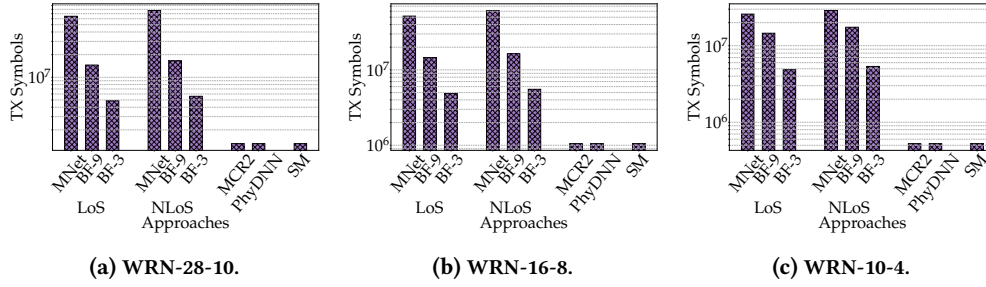


**Figure 12: Communication load comparison.** The plots show the total number of transmitted I/Q symbols (payload and overhead combined) for different DNNs.

methods on average with WRN-10-4, and reduces computation energy by  $33.97\times$  compared to task-oriented SemCom approaches on average with WRN-28-10. Even in the most demanding case (WRN-28-10 under NLoS), Semantic Multiplexing remains significantly more efficient, with a total energy usage well below all baselines ( $11.36\times$  lower than MNet/ms which is the second best method). This efficiency stems from Semantic Multiplexing’s strategic computation distribution, where only the first layer and the lightweight precoding are executed on the mobile device, while the energy-intensive deeper layers are offloaded to the edge server. Furthermore, its efficiency gain arises from task multiplexing, which reduces the average energy consumption per input.

**Communication and Computation Efficiency.** The total number of transmitted I/Q symbols—including both payload and protocol overhead, measured for various approaches under both LoS and NLoS conditions, is depicted in Figures 12a–12c. Full protocol stack baselines exhibit the highest communication overhead, while Semantic Multiplexing maintains a near-constant transmission volume of just  $1.3 \times 10^6$  symbols regardless of the environment by bypassing all the overhead introduced by the different layers of the stack. On average, Semantic Multiplexing reduces the number of transmitted symbols by  $54.24\times$  compared to MNet/ms,  $16.73\times$  compared to BF-9/ss, and  $5.56\times$  compared to BF-3/ss across LoS/NLoS scenarios and models.

Table 4 reports the number of parameters and floating-point operations (FLOPs) required to execute the head DNNs across all evaluated methods and WideResNet architectures. While MCR2/sm exhibits the highest computational load at the transmitter—reaching over 36 MB and 5.3 billion MACs in WRN-28-10—other full-stack baselines also impose non-trivial memory and compute overhead. Semantic Multiplexing guarantees high task performance (as shown in Table 1) with a substantially lower computational and memory footprint. For instance, in WRN-10-4, it requires 42.9 KB of memory and 13.2 MMac, which is significantly lower than all

**Table 4: Memory and computational load of the head DNN on the mobile device.**

	MNet	BF	MCR2	PhyDNN	SM
<b>WRN-28-10</b>					
Params	100	719	36474	1642	216
FLOPs	47	875	5399	1830	92
<b>WRN-16-8</b>					
Params	66	328	10957	464	67
FLOPs	27	389	1612	536	40
<b>WRN-10-4</b>					
Params	5	15	1795	48	5
FLOPs	3	28	275	65	7

baselines. Even in deeper architectures like WRN-28-10, Semantic Multiplexing keeps its computation below 100 MMac and memory footprint under 0.5 MB.

**Adaptation to Dynamic Channels.** We simulated a dynamic wireless channel by changing the positions of the transmitter and receiver every 100 inference steps, resulting in new CSI realizations. Classification accuracy on CIFAR-10 using WRN-28-10 is recorded continuously to assess each method’s ability to maintain task performance under these variations. As shown in Figure 13, Semantic Multiplexing maintains consistently high accuracy throughout the adaptation sequence, while MCR2/sm exhibits frequent and severe drops in performance. This discrepancy stems from the fact that MCR2/sm depends on an iterative precoding algorithm that solves an optimization problem for each new CSI snapshot. However, this approach introduces instability, especially when the channel varies quickly, and leads to significant task performance degradation. In contrast, Semantic Multiplexing employs a stochastic, learnable precoder to handle dynamic channel conditions. By incorporating randomness into its design, the precoder compensates for the channel distortions and enables generalization across diverse environments ensuring stable performance without runtime overhead. Quantitatively, Semantic Multiplexing achieves an average classification accuracy of 92.56% over 500 adaptation steps, with a minimum of 91.55% and a maximum of 93.33%. In contrast, MCR2/sm accuracy is on average only 85.88%, with drops down to 80.33%.

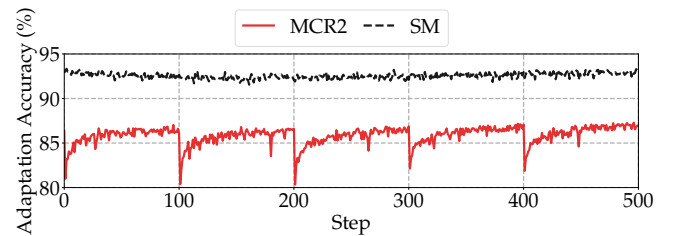


**Figure 13: Comparison between Semantic Multiplexing and MCR2/sm in inference-time adaptation to varying channels.**



## 6 Related Work

While the goal of the first SemCom systems was the exact recovery of the transmitter (input) message or its semantics at the receiver (output), later studies replaced the reconstruction loss with a task loss to achieve task-oriented SemCom [25, 31]. The authors in [12] proposed a joint source and channel coding (JSCC) scheme by using an autoencoder architecture with a noise-injection layer that models the wireless channel, and train it for an image retrieval task. In [1], the authors propose a task-oriented SemCom system that generates discrete latent symbols to be directly modulated and transmitted as a waveform. They take an already-trained DNN and fine-tune it considering the channel distortions so that it can be brought to the PHY layer. However, the proposed system only supports single-input single-output (SISO) communication and fails to exploit the high communication rates enabled by MIMO communication systems. The utilization of MIMO transceivers has been investigated in [29, 30, 33] by directly reusing traditional MIMO techniques. However, such designs focus on communication metrics such as throughput maximization, mean-square error (MSE) and bit error rate (BER) minimization, which are inconsistent with task performance goals [28]. Cai et al. [5, 6] used maximal coding rate reduction as a substitute objective for the end task performance to train the MIMO system. They proposed a DNN-based algorithm to optimize the linear precoding and postcoding blocks adopted in their system. However, they optimize the wireless communication and the DNN-based codecs separately. Such design cannot achieve an end-to-end optimal system where both communication and computation are learned with the aim of successful task completion. Moreover, approaches in the literature are unable to multiplex computation and transmission of more computing tasks than the number of physically available channels.

## 7 Conclusions and Next Steps

In this work, we have proposed *Semantic Multiplexing*, a new SemCom strategy to jointly process and transmit several computing tasks at the semantic layer. Semantic Multiplexing addresses the key bottleneck of current approaches being the separate optimization of the communication and computation pipelines which notoriously requires a complicated design. For this, we analytically formulate a probabilistic model of the transmitter and receiver system and trained it in a task-oriented fashion. A precoder and postcoder are designed to allow the transmitter and receiver to compensate for the wireless channel impairments. To enable the joint optimization of the communication and computation objectives, we developed and integrated a wireless channel model into the system. We developed a semantic channel sounding strategy on top of the standard sounding to make the

Semantic Multiplexing modules adapt to the varying channel conditions. We prototyped Semantic Multiplexing on an experimental and extensively evaluated its performance on image classification and sentiment analysis.

Our experimental results have shown that Semantic Multiplexing outperforms state-of-the-art SemCom approaches allowing the system to semantically multiplex more tasks than the number of physical streams. We believe our study may open several exciting research avenues in the field of semantic networking. For example, an intriguing direction would be investigating the tradeoffs at the basis of semantic multiplexing and its optimization depending on the specific applications. We have experimentally shown in Section 5.2 that multiplexing performance changes based on the specific task and the approach to address it (semantic processing). We also revealed that the design of the disjoint processing before binding the input tasks also impacts the performance. While in our study we started evaluating these tradeoff between performance and computational complexity experimentally, future research may target a further analytical analysis of these design parameters to investigate these tradeoff at a fundamental level. Indeed, the upper bound on the number of tasks that can be multiplexed based on the problem constraints is an open and intriguing research question triggered by the new semantic communication approach we proposed in this paper.

## References

- [1] Mohammad Abdi, Khandaker Foysal Haque, Francesca Meneghello, Jonathan Ashdown, and Francesco Restuccia. 2025. PhyDNNs: Bringing Deep Neural Networks to the Physical Layer. *Proceedings of IEEE International Conference on Computer Communications (INFOCOM)* (2025).
- [2] Alexander A Alemi, Ian Fischer, Joshua V Dillon, and Kevin Murphy. 2016. Deep Variational Information Bottleneck. *arXiv preprint arXiv:1612.00410* (2016).
- [3] Apple Inc. 2025. Apple Vision Pro. Product page. <https://www.apple.com/apple-vision-pro/> Accessed: 2025-08-30.
- [4] David M Blei, Alp Kucukelbir, and Jon D McAuliffe. 2017. Variational Inference: A Review for Statisticians. *Journal of the American statistical Association* 112, 518 (2017), 859–877.
- [5] Chang Cai, Xiaojun Yuan, and Ying-Jun Angela Zhang. 2024. Multi-Device Task-Oriented Communication via Maximal Coding Rate Reduction. *IEEE Transactions on Wireless Communications* 23, 12 (2024), 18096–18110. <https://doi.org/10.1109/TWC.2024.3461336>
- [6] Chang Cai, Xiaojun Yuan, and Ying-Jun Angela Zhang. 2025. End-to-End Learning for Task-Oriented Semantic Communications Over MIMO Channels: An Information-Theoretic Framework. *IEEE Journal on Selected Areas in Communications* (2025).
- [7] Maria Gallagher and Elisa Raffaella Ferrè. 2018. Cybersickness: a Multisensory Integration Perspective. *Multisensory research* 31, 7 (2018), 645–674.
- [8] Stephen I Gallant and T Wendy Okaywe. 2013. Representing Objects, Relations, and Sequences. *Neural Computation* 25, 8 (2013), 2038–2078.
- [9] Giovanni Geraci, Francesca Meneghello, Francesc Wilhelmi, David Lopez-Perez, Iñaki Val, Lorenzo Galati Giordano, Carlos Cordeiro,

- Monisha Ghosh, Edward Knightly, and Boris Bellalta. 2025. Wi-Fi: Twenty-Five Years and Counting. *arXiv preprint arXiv:2507.09613* (2025).
- [10] Andrea Goldsmith. 2005. *Wireless Communications*. Cambridge Univ. Press.
- [11] Cheongjae Jang, Sungyoon Lee, Frank Park, and Yung-Kyun Noh. 2022. A reparametrization-invariant sharpness measure based on information geometry. *Advances in neural information processing systems* 35 (2022), 27893–27905.
- [12] Mikolaj Jankowski, Deniz Gündüz, and Krystian Mikolajczyk. 2020. Wireless Image Retrieval at the Edge. *IEEE Journal on Selected Areas in Communications* 39, 1 (2020), 89–100.
- [13] Ian H Jermyn. 2005. Invariant Bayesian estimation on manifolds. (2005).
- [14] Yiping Kang, Johann Hauswald, Cao Gao, Austin Rovinski, Trevor Mudge, Jason Mars, and Lingjia Tang. 2017. Neurosurgeon: Collaborative Intelligence Between the Cloud and Mobile Edge. *ACM SIGARCH Computer Architecture News* 45, 1 (2017), 615–629.
- [15] Diederik P Kingma, Max Welling, et al. 2013. Auto-encoding variational bayes.
- [16] Denis Kleyko, Dmitri A Rachkovskij, Evgeny Osipov, and Abbas Rahimi. 2022. A survey on hyperdimensional computing aka vector symbolic architectures, part i: Models and data transformations. *Comput. Surveys* 55, 6 (2022), 1–40.
- [17] Huanghuang Liang, Qianlong Sang, Chuang Hu, Dazhao Cheng, Xiaobo Zhou, Dan Wang, Wei Bao, and Yu Wang. 2023. DNN surgery: Accelerating DNN inference on the edge through layer partitioning. *IEEE transactions on Cloud Computing* 11, 3 (2023), 3111–3125.
- [18] Andrew L. Maas, Raymond E. Daly, Peter T. Pham, Dan Huang, Andrew Y. Ng, and Christopher Potts. 2011. Learning Word Vectors for Sentiment Analysis. In *Proceedings of the 49th Annual Meeting of the Association for Computational Linguistics: Human Language Technologies*, Dekang Lin, Yuji Matsumoto, and Rada Mihalcea (Eds.). Association for Computational Linguistics, Portland, Oregon, USA, 142–150. <https://aclanthology.org/P11-1015/>
- [19] Yoshitomo Matsubara, Davide Callegaro, Sameer Singh, Marco Levorato, and Francesco Restuccia. 2022. BottleFit: Learning Compressed Representations in Deep Neural Networks for Effective and Efficient Split Computing. In *Proceedings of IEEE International Symposium on a World of Wireless, Mobile and Multimedia Networks (WoWMoM)*.
- [20] Nicolas Menet, Michael Hersche, Geethan Karunaratne, Luca Benini, Abu Sebastian, and Abbas Rahimi. 2023. MIMONets: Multiple-Input-Multiple-Output Neural Networks Exploiting Computation in Superposition. *Advances in Neural Information Processing Systems* 36 (2023), 39553–39565.
- [21] Thaha Mohammed, Carlee Joe-Wong, Rohit Babbar, and Mario Di Francesco. 2020. Distributed Inference Acceleration with Adaptive DNN Partitioning and Offloading. In *Proceedings of IEEE Conference on Computer Communications (INFOCOM)*. IEEE, 854–863.
- [22] Vishvak Murahari, Ameet Deshpande, Carlos E Jimenez, Izhak Shafran, Mingqiu Wang, Yuan Cao, and Karthik Narasimhan. 2023. Mux-plms: Data multiplexing for high-throughput language models. *arXiv preprint arXiv:2302.12441* (2023).
- [23] Vishvak Murahari, Carlos Jimenez, Runzhe Yang, and Karthik Narasimhan. 2022. DataMUX: Data Multiplexing for Neural Networks. *Advances in Neural Information Processing Systems* 35 (2022), 17515–17527.
- [24] Tony A Plate. 1995. Holographic Reduced Representations. *IEEE Transactions on Neural networks* 6, 3 (1995), 623–641.
- [25] Jiawei Shao, Yuyi Mao, and Jun Zhang. 2021. Learning Task-Oriented Communication for Edge Inference: An Information Bottleneck Approach. *IEEE Journal on Selected Areas in Communications* 40, 1 (2021), 197–211.
- [26] Yi Tay, Mostafa Dehghani, Samira Abnar, Yikang Shen, Dara Bahri, Philip Pham, Jinfeng Rao, Liu Yang, Sebastian Ruder, and Donald Metzler. 2021. Long Range Arena : A Benchmark for Efficient Transformers. In *International Conference on Learning Representations*. <https://openreview.net/forum?id=qVyeW-grC2k>
- [27] Naftali Tishby, Fernando C Pereira, and William Bialek. 2000. The information bottleneck method. *arXiv preprint physics/0004057* (2000).
- [28] Dingzhu Wen, Xiang Jiao, Peixi Liu, Guangxu Zhu, Yuanming Shi, and Kaibin Huang. 2023. Task-Oriented Over-the-Air Computation for Multi-Device Edge AI. *IEEE Transactions on Wireless Communications* 23, 3 (2023), 2039–2053.
- [29] Haotian Wu, Yulin Shao, Chenghong Bian, Krystian Mikolajczyk, and Deniz Gündüz. 2024. Deep Joint Source-Channel Coding for Adaptive Image Transmission Over MIMO Channels. *IEEE Transactions on Wireless Communications* 23, 10 (October 2024), 15002–15017.
- [30] Huiqiang Xie, Zhijin Qin, Xiaoming Tao, and Khaled B Letaief. 2022. Task-Oriented Multi-User Semantic Communications. *IEEE Journal on Selected Areas in Communications* 40, 9 (2022), 2584–2597.
- [31] Songjie Xie, Shuai Ma, Ming Ding, Yuanming Shi, Mingjian Tang, and Youlong Wu. 2023. Robust Information Bottleneck for Task-Oriented Communication with Digital Modulation. *IEEE Journal on Selected Areas in Communications* 41, 8 (2023), 2577–2591.
- [32] Sergey Zagoruyko and Nikos Komodakis. 2016. Wide Residual Networks. In *British Machine Vision Conference 2016*. British Machine Vision Association.
- [33] Guangyi Zhang, Qiyu Hu, Yunlong Cai, and Guanding Yu. 2024. SCAN: Semantic Communication with Adaptive Channel Feedback. *IEEE Transactions on Cognitive Communications and Networking* 10, 5 (October 2024), 1759–1773.

## Appendix

### A Variational Upper Bound and Loss Function Computation

In this section, we derive an approximation of the loss function in Equation (2) that can be effectively implemented to jointly train the Semantic Multiplexing modules. This is required as computing the distributions  $p(z)$  and  $p(y|z, s)$  for high-dimensional data with arbitrary distributions is computationally prohibitive.

**Variational Upper Bound Reformulation.** We define two variational distributions  $q(z)$  and  $q(y|z, s)$  to approximate  $p(z)$  and  $p(y|z, s)$ . Specifically, we take the postcoder together with the receiver processing block to be the variational approximation of  $p(y|z, s)$ . The type of this conditional probability  $p(y|z, s)$  depends on the task. For example, for classification tasks, it has a categorical distribution, and its parameters are found using the postcoder together with the receiver processing. Using this approximation, the variational upper bound of the first term in Equation (2) is obtained as

$$\begin{aligned}
\mathbb{E}_{p(x,y)} \left\{ \mathbb{E}_{p(\hat{z}|x,s)} [-\log p(y|\hat{z},s)] \right\} &= \\
\mathbb{E}_{p(x,y)} \left\{ \mathbb{E}_{p(\hat{z}|x,s)} [-\log q(y|\hat{z},s)] \right\} & \\
- \underbrace{\mathbb{E}_{p(\hat{z})} \left\{ \mathbb{E}_{p(y|\hat{z},s)} \left[ \log \frac{p(y|\hat{z},s)}{q(y|\hat{z},s)} \right] \right\}}_{D_{KL}(p(y|\hat{z},s)||q(y|\hat{z},s)) \geq 0} & \\
\leq \mathbb{E}_{p(x,y)} \left\{ \mathbb{E}_{p(\hat{z}|x,s)} [-\log q(y|\hat{z},s)] \right\}. &
\end{aligned}$$

Similarly, we compute the upper bound for the second term in Equation (2) as

$$\begin{aligned}
D_{KL}(p(z|x,s)||p(z)) &= D_{KL}(p(z|x,s)||q(z)) \\
&\quad - \underbrace{D_{KL}(p(z)||q(z))}_{\geq 0} \\
&\leq D_{KL}(p(z|x,s)||q(z)).
\end{aligned}$$

Since minimizing this upper bound minimizes the KL divergence between  $p(z|x,s)$  and  $q(z)$ , a certain variational prior  $q(z)$  can be imposed to induce that prior distribution on the latent symbols. Therefore, to regularize (sparsify) the latent space during training and prevent Semantic Multiplexing from memorizing an exact mapping, we use a standard complex normal prior distribution i.e.,  $q(z) \sim \mathcal{CN}(\mathbf{0}, \mathbf{I})$ .

In conclusion, the variational upper bound of the loss function in Equation (2) writes as

$$\begin{aligned}
\mathcal{L}_{VIB} &= \mathbb{E}_{p(x,y)} \left\{ \mathbb{E}_{p(s)} \left\{ \mathbb{E}_{p(\hat{z}|x,s)} [-\log q(y|\hat{z},s)] \right. \right. \\
&\quad \left. \left. + \beta \cdot D_{KL}(p(z|x,s)||\mathcal{CN}(\mathbf{0}, \mathbf{I})) \right\} \right\}. \tag{3}
\end{aligned}$$

As  $p(z|x,s)$  is assumed to be Gaussian and the KL divergence between two complex Gaussian distributions has a closed-form expression, the second term in Equation (3) can be computed analytically.

**Monte Carlo Sampling.** Monte Carlo sampling can be used to obtain an unbiased estimate of the expected values in Equation (3). Semantic Multiplexing is trained using a gradient descent algorithm on the estimated loss. Note that the precoder output is a distribution, and it should be sampled to obtain a realization. However, such sampling is not differentiable. Therefore, we use the reparameterization trick [15] to make Semantic Multiplexing trainable through loss backpropagation. More in detail, given a mini-batch of  $N_{mb} \times N_{comp}$  data points  $\{(x_i, y_i)\}_{i=1}^{N_{mb} \times N_{comp}}$ , where  $N_{mb}$  is the batch size and  $N_{comp}$  is the number of multiplexed task inputs, we feed  $N_{comp}$  inputs  $x$  to the transmitter processing plus the precoder and the Gaussian distribution parameters are obtained for latent symbols in each packet and subcarrier  $z_{p,k}$ . Then,  $N_{mc}$  realizations of latent symbols  $z$ , where  $N_{mc}$  is the number of Monte Carlo samples, are sampled using these

distributions. Also,  $N_{mc}$  realizations of the CFR and  $N_{mc}$  realizations of the channel noise  $n^f$  are sampled to define  $N_{mc}$  realizations of the CSI ( $s$ ). Hence, the Semantic Multiplexing loss function is estimated as follows

$$\begin{aligned}
\tilde{\mathcal{L}}_{VIB} &= \frac{1}{N_{mb}} \sum_{n_{mb}=1}^{N_{mb}} \left\{ \frac{1}{N_{mc}} \sum_{n_{mc}=1}^{N_{mc}} [-\log q(y_{n_{mb}}|\hat{z}_{n_{mb},n_{mc}})] \right. \\
&\quad \left. + \beta \cdot \sum_{p=1}^P \sum_{k=1}^K D_{KL}(p(z_{n_{mb},n_{mc},p,k}|x_{n_{mb}},s_{n_{mc}})||\mathcal{CN}(\mathbf{0}, \mathbf{I})) \right\}, \tag{4}
\end{aligned}$$

where  $\hat{z}_{n_{mb},n_{mc}} = H_{n_{mc}} z_{n_{mb},n_{mc}} + n_{n_{mc}}^f$ .

## B Accuracy on CIFAR-100 and SVHN

We report the image classification accuracy using the CIFAR-100 and SVHN datasets in Tables 5-6. We compare the performance of Semantic Multiplexing with the other baselines for all the three DNN models considered for this task. The results are in line with the discussion in Section 5.1: Semantic Multiplexing lead to a slight degradation in performance with respect to the full protocol stack approaches while surpassing all PHY strategies. Moreover, by comparing the results in a cross-dataset fashion, we can see that the multiplexing performance depends on the task complexity, e.g, recognizing images from 10 classes (CIFAR-10, SVHN) or from 100 classes (CIFAR-100), as discussed in Section 5.2. We remind that the performance of full-stack approaches is not affected by the communication scenario.

**Table 5: Image classification. Experimental evaluation of Semantic Multiplexing and baselines for different DNNs on CIFAR-100.**

WRN-28-10	MNet	BF-9	BF-3	MCR2	PhyDNN	SM
LoS	79.20 %	81.32 %	80.63 %	74.68 %	75.75 %	78.87 %
NLoS				71.46 %	72.52 %	76.62 %
WRN-16-8	MNet	BF-9	BF-3	MCR2	PhyDNN	SM
LoS	76.84 %	77.58 %	77.12 %	71.87 %	72.74 %	75.13 %
NLoS				68.14 %	69.30 %	72.31 %
WRN-10-4	MNet	BF-9	BF-3	MCR2	PhyDNN	SM
LoS	66.23 %	69.08 %	67.38 %	60.55 %	61.43 %	63.58 %
NLoS				58.42 %	59.88 %	61.14 %

**Table 6: Image classification. Experimental evaluation of Semantic Multiplexing and baselines for different DNNs on SVHN.**

<b>WRN-28-10</b>	MNet	BF-9	BF-3	MCR2	PhyDNN	<b>SM</b>
LoS						
NLoS	96.88 %	97.11 %	97.08 %	92.48 % 90.02 %	94.92 % 92.68 %	96.51 % 94.73 %
<b>WRN-16-8</b>	MNet	BF-9	BF-3	MCR2	PhyDNN	<b>SM</b>
LoS						
NLoS	96.69 %	96.84 %	96.67 %	92.45 % 89.40 %	95.27 % 92.97 %	96.32 % 94.91 %
<b>WRN-10-4</b>	MNet	BF-9	BF-3	MCR2	PhyDNN	<b>SM</b>
LoS						
NLoS	94.33 %	94.84 %	94.53 %	91.14 % 89.02 %	92.67 % 90.80 %	93.61 % 92.12 %